Design of a Hypergravity Simulation Platform with Speed and Axis Stability Control Systems

Matthew Joseph Dionela[1,*], Jasper Matthew Tan[1], Louise Marwin Paran[1], Ronnie Concepcion II[1], Argel Bandala[2], Luigi Gennaro Izzo[3]
[1]*Department of Manufacturing Engineering and Management, De La Salle University*, Manila, Philippines
[2]*Department of Electronics and Computer Engineering, De La Salle University*, Manila, Philippines
[3]*Department of Agricultural Sciences, University of Naples Federico II*, Portici, Italy
{matthew_dionela*, jasper_matthew_tan, louise_paran, ronnie.concepcion, argel.bandala}@dlsu.edu.ph, luigigennaro.izzo@unina.it

2022 IEEE 14th International Conference on Humanoid, Nanotechnology, Information Technology, Communication and Control, Environment, and Management (HNICEM) | 978-1-6654-6493-2/22/$31.00 ©2022 IEEE | DOI: 10.1109/HNICEM57413.2022.10109584

***Abstract*—Plant growth in space is imperative for food consumption by astronauts during long term space missions. These plants are being grown in bioregenerative life support systems (BLSS), designed to support life while withstanding space conditions. Its research is still commonly done in space stations, and there are still limited studies available about ground-based BLSS. One of the dominantly experienced conditions during space missions is the varied gravity levels such as hypergravity, where gravitational accelerations are higher than that of Planet Earth. Hypergravity is usually simulated through centrifuges that rotate at high speeds. However, no studies have focused yet on providing control systems for more stable simulations of these rotational speeds. Hence, this study designed a hypergravity platform speed and axis control system (HPSACS) and characterized it in terms of maximum motor speed, torque, and sensor placements. The speed control system contains an in-depth design and elucidation with graphs for a transfer function to control the speed output of the motor, while the axis stability control system was analyzed in terms of its components and working principle. After all necessary calculations and graphing, the results have shown that the transfer function's graph was undamped and the most suitable for the speed stability system is the step input with I compensation, s^{-1}, for the elimination of steady-state error and consistent amplitude in the graph simulation.**

Keywords—bioregenerative life support systems, centrifuge, control systems, hypergravity, simulated gravity, system analysis

I. Introduction

Bioregenerative life support systems (BLSS) are a relatively new area of study for the purpose of sustaining and regenerating food products for space exploration, particularly for astronauts on long-term space missions. BLSS are known to enable the preparation and storage of food products that aid astronauts to stay in a healthy condition despite stressful conditions in space [1, 2]. To produce food, BLSS mainly allow the growth of crops under space conditions, until edible harvest can be consumed. However, to date, the growth behavior of plants in space is a relatively new research field that is still being advocated and recommended for researchers to pursue given that there is only limited research available. Moreover, critical assessments from space experiment results are necessary and highly encouraged to conduct since these experiments often have specific restricted conditions [3]. But another issue is that such experiments are usually done at space stations at low earth orbit (LOE), to which there are only two actives to date [4, 5]. This poses the need to make the studying of crop growth behavior in space more accessible on Earth, which can be addressed by developing an Earth-based or ground-based BLSS simulator for crop growth. This implies that ground-based BLSS need to simulate space gravity conditions.

The concept of gravity is one that is tied to the planet Earth. The Earth enables any being or object to be held on the surface due to gravitational field or force [6]. According to Newton's Law, the acceleration due to gravity on Earth is g = 9.8 $m \cdot s^{-2}$ [7]. But in outer space, gravity is different and thus the g-values vary. When gravity experienced is higher than the g-value on Earth, it is called "hypergravity", commonly denoted as ">1g" [8, 9]. Hypergravity can be experienced in different regions in space and in some planets in our solar system: Jupiter (2.53g), Saturn (1.07g), and Neptune (1.14g) [10]. Moreover, hypergravity is experienced during launch ($\approx$3.2g) and reentry ($\approx$1.4g) with spacecraft flights [8]. These are some cases that highlight the importance of hypergravity studies in the context of BLSS, more specifically for studying crop growth in space. Hypergravity is one of the direct recommendations for research by [3] so that plant growth studies in space can be as standardized as possible in following space conditions.

A study focused on the physiological changes on *Physcomitrella patens* plant after ground-based hypergravity experiments. It was found out that gravity affects the growth of crops in their direction of growth and shape, and that crops adjust their other phenotypic traits as a type of resistance response to various gravitational forces [11]. Another study used a Large Diameter Centrifuge for hypergravity simulations of up to 20g while observing Brassica oleracea plant growth, but also testing the effects of light. This study then focused on both gravitropism and phototropism, both of which were proven to affect the curvature of the seedlings' roots [12]. Hypergravity was established to have favorable effects on the growth of crops through centrifugal simulations, one study of which investigated the germination rate of maize at its early stages of growth at various g-values. This study concluded that a centrifugal force of greater than 1g does lead to a positive effect on the germination rate of the maize crop [13]. Another study explained the molecular basis of their observation that the root growth phenotype of their bread wheat plant had a significant increase after hypergravity simulations at 10g for 12 hours. They have also found out that the cell division, hormonal responses, and cell wall characteristics were enriched from hypergravity treatments [14]. There are also studies that discuss how hypergravity, as opposed to microgravity (<1g), is more beneficial for both plants and human health in space [15, 16]. A study on *Arabidopsis thaliana* found out that microgravity significantly degraded cell growth and proliferation in the crop being grown [15]. Aside from this, microgravity was found out to cause bone density loss significantly, and that artificial centrifugation or hypergravity is a countermeasure against such losses [16]. The previously mentioned studies all the more enhance the significance of studying hypergravity effects on crop growth, as it is also a significant potential case where hypergravity must be experienced in long-term space missions by both crops and astronauts in the spacecraft.

The commonality among these studies is having the means to enable centrifugal force and motion through rotations

at high speeds through centrifugal machines. One study designed a medical centrifuge with servo control system in order to control its electromagnetic torque, including speed, to optimize the overall quality of rotations for more accurate medicinal research. The optimized system of this study was achieved through the help of a fuzzy neural network and proportional integral (PI) controller [17]. Another study emphasized on the application of centrifugal machines in manufacturing, particularly for sugar. It was mentioned that in order to maintain sugar quality, reference states of its machine must be accounted for, thus needing a speed controller which the researchers of the study had developed [18]. The problem presented by both studies, one way or another, is about maintaining the accuracy of speed of their motors for quality results. Fluctuations in speed output of motors can be caused by varying loads applied and voltage fluctuations [19]. The hypergravity platform designed for this study is also prone to such problems. Varying loads may occur since throughout the fertigation of a plant, water will be injected into the soil and can evaporate at times, and the growth of seedlings may vary per chamber. The effects on these are random with regards to weight, hence possible variations in loads. As for voltage, if no control is given, any motor has the tendency to fluctuate due to undesired harmonics or noise, affecting the overall output which is speed and also the stability of the axis of rotation [20, 21].

In response to the mentioned problems, the objective of this study is to design a hypergravity platform speed and axis control system (HPSACS) for the purpose of biological research, specifically on determining plant growth characteristics under the influence of hypergravity. This objective was first met by determining the torque of the centrifuge by establishing the maximum rotation speed for the platform then selecting an appropriate motor model with a torque specification. From there, a computer aided design (CAD) model was made for the centrifuge to allow visualization of its components, sensor-placements, and intended working principles. Finally, the control system for speed was formulated mathematically through an appropriate transfer function with graphs generated through MATLAB, tested with step, ramp, and parabolic inputs with incorporation of P and I compensations. Steady-state values and errors, time constant, rise time, and settling time were also shown for each case. Likewise, natural frequency, damping ratio, peak time, settling time, and percent overshoot of the transfer function graph was both calculated and displayed. As for the axis stability control system, its components and basic working principle with an angle sensor was also discussed. It should be noted however that the maximum load capacity testing and in-depth discussion of the sensor setups are out of scope for this study. Both of these will be explored in future studies by the researchers as they pursue the fabrication of the proposed hypergravity platform.

Nonetheless, this current study will contribute the following: (1) discussions in the newly-growing research field of earth-based BLSS for optimal crop growth for long-term space explorations with a focus on stable simulations of hypergravity; (2) provision of a system concept for controlling the speed and axis stability of a centrifuge motor for hypergravity; and (3) provision of clear mathematical models and discussions for the mentioned control system which can be replicated and adopted for future hypergravity studies utilizing centrifuge motors.

II. Hypergravity Platform Design

A. Motor Selection - Maximum Motor Speed Calculation & Torque Determination

For the calculations, the first important quantity that the researchers determined was the g-value. The hypergravity platform is aimed to study the crop growth behaviors at the common cases of hypergravity mentioned such as planets with g-values greater than 1 [10] as well as launch and reentry of a spacecraft [8]. But to consider a higher possible g-value simulatable for future researchers using the proposed design, the researchers considered the maximum g-value from [12], which was 20g. Thus, a g-value of 25g was selected for allowance. Next, the rotor speed required to simulate the 25g hypergravity had to be solved. Eq. (1) [22] shows the derived equation to solve the rotor speed in rpm with radial distance (r) since the g-value, or relative centrifugal force (RCF), is already known for the case of this research.

$$rpm = \sqrt{\frac{RCF}{(11.18)(r)}}\,(1000) \tag{1}$$

Through utilizing (1) and an r-value of 77.47 cm determined through the proposed design's CAD model (Fig. 1), the computed rotor speed value was 169.896 rpm, which can be rounded up to 170 rpm. With this speed, the researchers were able to find a suitable motor that can rotate at the said speed. To be specific, the motor model chosen was the Yanmis AC Gear Motor, 220V 6W asynchronous motor M206-402, single phase, 4-poles, which comes with a governor for adjusting motor speed [23]. From its specifications, the researchers were able to determine that the maximum torque of the motor model at 170 rpm is 0.36 Newton-meters.

B. Visualization of the Hypergravity Platform Through CAD

The proposed hypergravity platform is based on The European Space Agency's ESTEC Large Diameter Centrifuge [24]. The CAD model can be seen in Fig. 1. The main parts of the platform include the four growth chambers, the arm base where the growth chambers are connected, the base, a belt drive, and the top housing. The chambers are made out of 3D printed material, having an overall dimension of 1.25 ft x 1ft x 1.44 ft. The arm base has a radius of 2.5 ft, being made from 3 in square metal tubing. The chambers are affixed to the arm base with the use of bolts and fasteners. The base is connected to the arm base via a shaft, having an octagonal base. The belt drive is located within the base itself, being connected to the shaft. The top housing contains the control system for the platform. The specific materials, fasteners, dimensions for the base, and shaft diameter are to be determined in the future with the utilization of FEA. The sensors to be used are speed and angle sensors, which will be placed at the base itself, and at the outside of the growth chambers respectively.

III. Hypergravity Platform Speed and Axis Control System (HPSACS)

A. Development of the Speed Stability Control System

The hypergravity platform has four frames carrying the cultivation chambers that rotate within an axis for the chambers to experience simulated hypergravity using the centrifugal force produced by the asynchronous motor. The system will be operated with microcontrollers with graphical user interface where the desired hypergravity would be inputted. The relationship between hypergravity and angular velocity [25]

which will be measured using a speed sensor can be described by (2) where G is gravity level, m is the mass of chamber, r is radius, g is Earth's gravitational acceleration, and w is angular velocity.

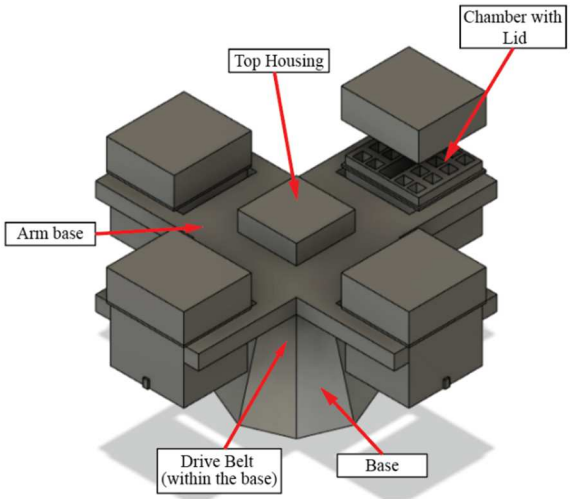

Fig. 1. Designed hypergravity platform CAD model in isometric view.

$$G = \frac{\sqrt{m^2r^2w^4+(mg)^2}}{mg} \quad (2)$$

The control system diagram in Fig. 2 shows the process on how the system flows. After inputting the desired hypergravity level, the microcontrollers will send a signal to the frequency converter and to the motor and start spinning. The speed sensor will then measure the angular velocity of the motor and send signals back to the system whether to increase or decrease the velocity output of the motor by adjusting the voltage and frequency it receives.

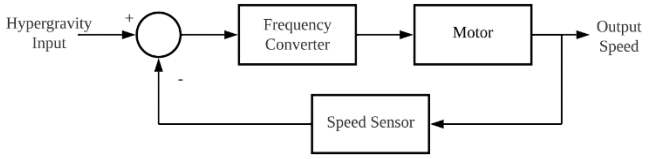

Fig. 2. Block diagram for the speed stability control system.

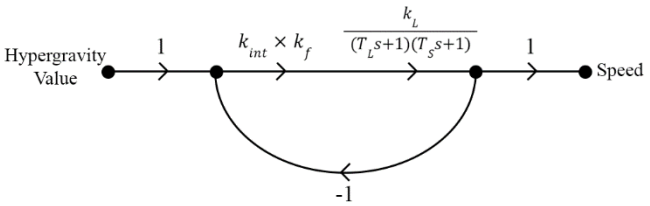

Fig. 3. Signal flow graph of speed stability system.

The frequency converter is used for the speed regulation of the AC motor as the motor is dependent on the frequency of the input current. AC motors or asynchronous motors generally have two inputs: voltage and frequency; and to control the speed of the motor, both inputs must be adjusted at the same time. As for the output of asynchronous motors, it is generally the motor speed and magnetic flux. By combining the frequency converter and the motor model which was simplified as a series of connected electrical links with a mechanical link based on the signal flow graph in Fig. 3, the transfer function of the system is shown in (3) where k_L is the motor gain factor, k_{int} is the voltage frequency coefficient, k_f is the conversion factor, T_L is the motor's mechanical time constant, and T_S is the motor's electrical time constant [26].

$$G(s) = \frac{k_L \times k_{int} \times k_f}{(T_L s+1)(T_S s+1)} \quad (3)$$

In this study, $k_L = 1$, $k_{int} \times k_f = 22$, $T_L = 0.012$s, and $T_S = 0.002$s. Considering that the system is a closed-loop second order system regulated with negative-unity feedback where H(s) = 1, the new transfer function is seen in (4).

$$G(s) = \frac{2750000}{3s^2+1750s+2875000} \quad (4)$$

The graph of the transfer function was tested in MATLAB using Gigabyte Aorus 5 Core i5-10200H. The transfer function was incorporated with step, ramp, and parabolic input and together with P compensation and I compensation to eliminate errors. In each input, the transfer function was graphed without any compensation, with P compensation K being equal to 10, 50, and 100, and with I compensation. The degree of the I compensation depends on the input of the function. For step input, only a single degree of I compensation, s^{-1} was tested. For ramp input, both first degree and second degree I compensation, s^{-2}, was tested. For parabolic input, second degree and third degree I compensation, s^{-3} were tested.

Another way to stabilize the output speed is with a PID controller that is incorporated in the system as seen in Fig. 6. For the PID, the focus is on the accurate output rather than the response time as the hypergravity platform will be used for weeks in performing BLSS experiments. This was simulated in MATLAB Simulink.

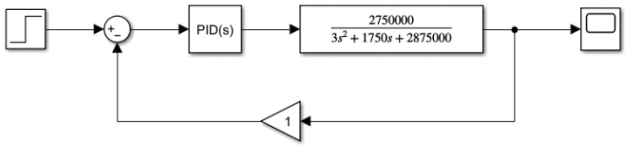

Fig. 4. Block diagram for speed control system with PID controller and transfer function.

For further analysis, steady-state error values have also been calculated with K_p which is the limit of G(s) as s approaches zero and $e_{ss} = (1+K_p)^{-1}$ for step input, K_v which is the limit of sG(s) as s approaches zero and $e_{ss} = K_v^{-1}$, for ramp input, and K_a which is the limit of $s^2G(s)$ as s approaches zero and $e_{ss} = K_a^{-1}$ for parabolic input. Other calculation also include the natural frequency, damping ratio, peak time, percent overshoot, settling time, and damping ratio calculated using $\omega_n = b^{1/2}$, $\zeta = a(2\omega_n)^{-1}$, $T_p = \pi[\omega_n(1-\zeta)^{½}]^{-1}$, $\%OS = e^{-[\zeta\pi/(1-\zeta)^{½}]}x100$, and $T_s = 4(\zeta\omega_n)^{-1}$ respectively. The basis equation of which the additional computations will come is as seen in (5).

$$s^2 + 583.333s + 958333.333 = 0 \quad (5)$$

B. Implementation of the Axis Stability Control System

The four frames carrying the cultivation chambers of the hypergravity platform have seeds growing in them, and the speed growth may vary depending on the set conditions on the chambers and thus resulting in varying weights. The uneven weight between the four chambers may cause the frames to tilt to the heavier side. As such, the system flowchart in Fig. 5 is designed to keep the weight equal between the four frames to maintain the perpendicularity of the rotation of the axis to the ground. Below are discussions on the other components that will possibly affect the uneven distribution of weights, which will be balanced by the axis stability control system.

1) Angle Sensor. Each frame is equipped with an angle sensor near the end to determine any deviations from the desired perpendicularity of the axis of rotation.

2) Water Reservoir. There will be one relatively large water reservoir at the center or the axis of rotation and another four at the end of each frame to balance the weight of all four frames. The reservoirs will be located within the frames and thus hidden from sight.

3) Control Valve. The control valve that allows or restricts the flow of water is a two-way valve so that delivering water from the center reservoir to the frame reservoir during the experiment and back to the center reservoir after the experiment is possible. The valve will be electrically actuated that allows water to flow to the end reservoir for 0.3 second whenever there is a detected imbalance of angle. Three seconds after the delivery of water and there is still a detected imbalance, the valve will be actuated again.

4) Water Hose. Water hose will be the pathway of water connecting the center reservoir to the control valve and to the end reservoir.

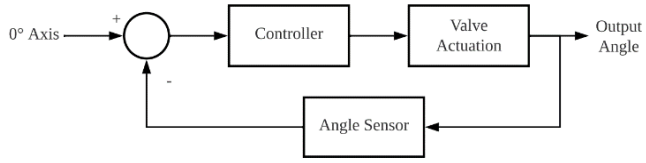

Fig. 5. Block diagram for the axis stability control system.

C. Sensor Placements

The speed sensor that will be used is a hall-effect sensor that utilizes the sensor itself, and a small magnet. The sensor will be placed 2-5 mm below the surface of the base, and 20 mm away from the base while the magnet will directly be connected to the arm base, and on top of the hall-effect sensor. The speed sensor placement can be seen in Fig. 6. Next, the angle sensor of the axis stability control system will be placed on the outside surfaces of each of the four growth chambers at the bottom as seen in Fig. 6. The method of controlling the weight is through the distribution of water within the frames. Whenever the four angle sensors placed in each frame read a degree other than zero, frames that are tilted upwards will receive additional weight through water. The readings from the angle sensor will detect the error in the system and the controller will open the valve for a given time allowing the water to flow through the hose. The water will have a reservoir in the center and at each end of the frames. The centrifugal force will deliver the water to the reservoir at the end of the frames whenever the valve is actuated.

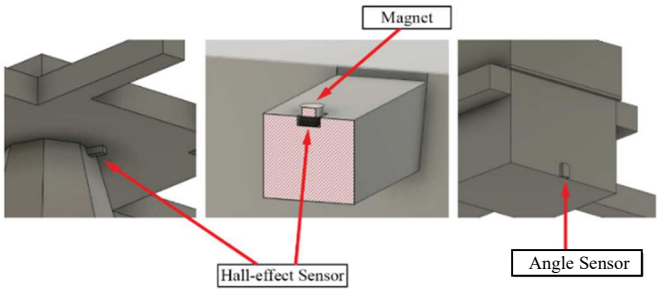

Fig. 6. Sensor placements on the customized hypergravity platform CAD model of the speed sensor and the hall-effect sensor.

IV. Results and Discussion

The transfer function for the speed stability system is a second-degree system with high natural frequency for its oscillation. The system is also considered to be underdamped as the damping ratio is between zero and one which is often the most practical to be used. However, it would be more ideal for the system to be a little bit more damped but still within the range of being underdamped because the overshoot percentage is quite large. The graph of the transfer function seen in Fig. 7 was also able to immediately reach the peak value and maintain the amplitude with 2% of the final value as the peak time and settling time are very short. The natural frequency, damping ratio, peak time, and percent overshoot in the graph were also calculated as second order system parameters of the transfer function and are summarized in Table I as supporting validation.

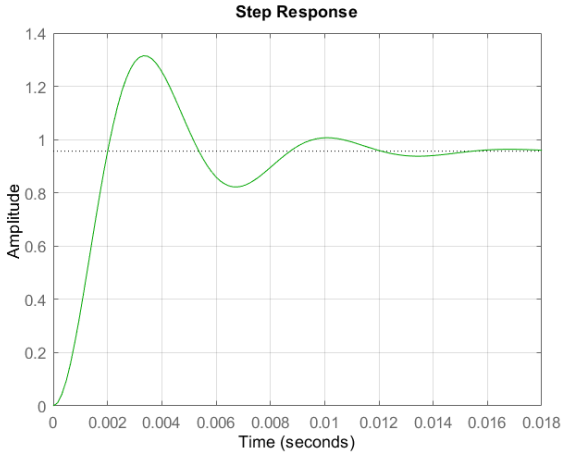

Fig. 7. Second Order System Responses

TABLE I. Second Order System Calculations for the Speed Control Transfer Function

Control Parameters	Value Calculated
Natural Frequency	978.945
Damping Ratio	0.2979
Peak Time	0.0034 s
Percent Overshoot	37.52%
Settling Time	0.0137 s

There were three main ways in which the control system for the speed was stabilized: using P compensation, I compensation, and PID controller. However, only P and I compensation have step, ramp, and parabolic inputs whereas the PID controller has only step input. For the step input, it was the I compensator that had no error and with minimal error for P compensation. However, in Fig. 8, it was the P compensator with K equal to 50 and 100 that is very close to the graph of I compensator with no error. For all types of inputs, the P compensation with K being equal to 50 and 100 were able to get close to the desired amplitude which is one but did not reach exactly the desired amplitude. By setting the graph to have an aim to reach an amplitude of one, the different inputs can now be rationalized. The graph of the transfer function in I compensation is also quite similar to the graph with the PID controller as to which the amplitude gradually increases. The graph of the transfer function with the PID controller is shown in Fig. 11 that shows that it reaches the desired amplitude precisely over a span of time. In the first second, the output remained zero, but it immediately achieved that desired output after it started rising although slightly fluctuating in its thousandths place. On the other hand, the second degree I

compensator for ramp input is the one with no error but has a wave-like behavior in Fig. 9. The P compensation with infinite steady-state error has higher amplitude compared to the single degree I compensator in which both have the same behavior. As for parabolic input, the third degree I compensator with zero error has a unique behavior in Fig. 10 whereas all other compensators whether with infinite or constant steady-state errors have similar behaviors. Overall, it was the step input I compensation that was the best stabilizer for the control system as it has no error and its smooth increase in amplitude would also be more beneficial to the motor because there would be no sudden change in speed thus experiencing less strain. There are also no fluctuations in the graph which give a very stable output. Furthermore, the hardware complexity that would be implemented would be significantly lower as compared to the compensation of ramp and parabolic input that has zero steady-state error.

The values for the rise time and peak time in this paper is significantly larger compared to a study using PID controller (Table 3). However, the optimization technique used in this paper has an ideal overshoot (Table 3). Also, the large rise and peak time are not necessarily detrimental in this system as an accurate response is more desirable rather than a quick response time. Therefore, I compensation employed in this study performed better based on the goal to have more accurate response and not fast convergence of response as it is more useful for hypergravity experiments. More advanced computational intelligence algorithms may be incorporated into perfecting the stability response for hypergravity platform [27,28].

TABLE II. STEADY-STATE ERROR OF THE TRANSFER FUNCTION PER INPUT TYPE AND COMPENSATION

Input	Compensation	Steady-State Error
Step	None	0.5111
	K = 10	0.0947
	K = 50	0.0205
	K = 100	0.0103
	1/s	0
Ramp	P compensation	∞
	1/s	1.0455
	$1/s^2$	0
Parabolic	P compensation	∞
	$1/s^2$	1.0455
	$1/s^3$	0

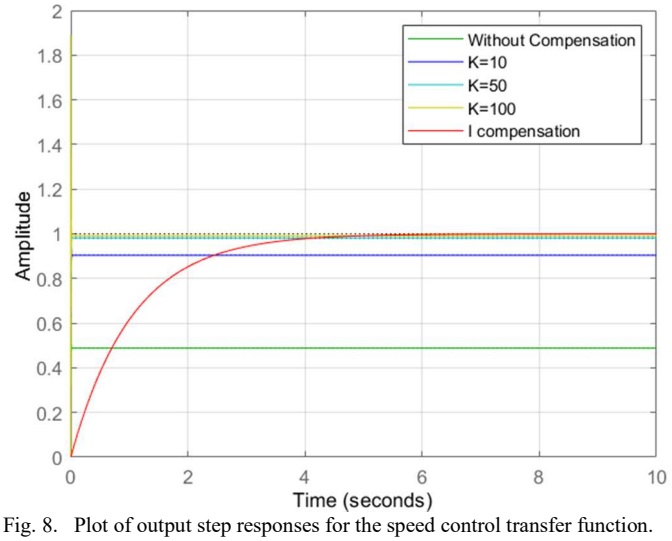

Fig. 8. Plot of output step responses for the speed control transfer function.

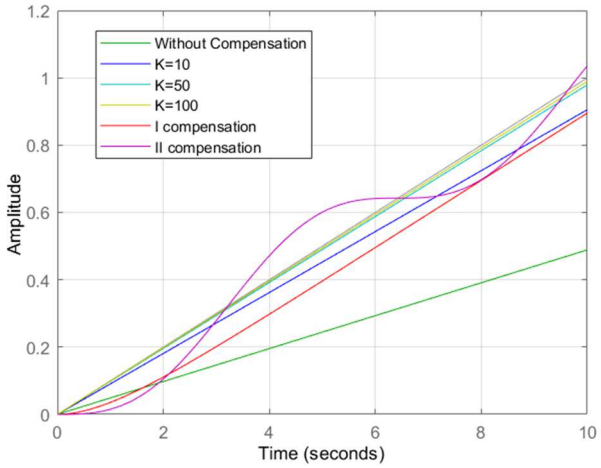

Fig. 9. Plot of output ramp responses for the speed control transfer function.

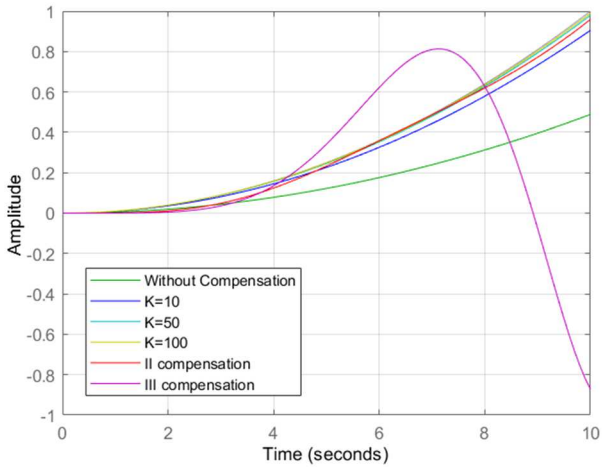

Fig. 10. Plot of output parabolic responses for the speed control transfer function.

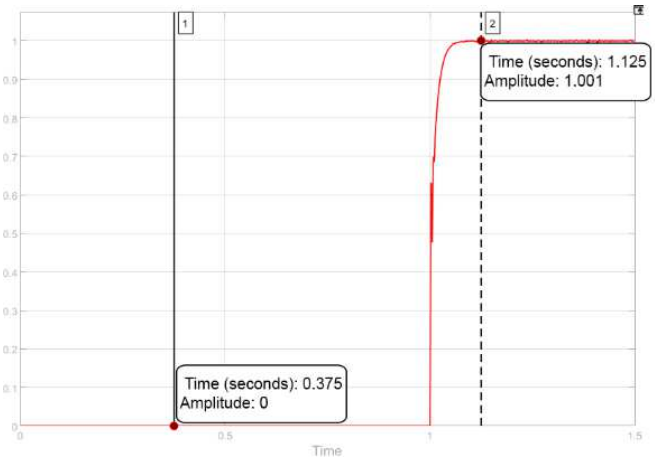

Fig. 11. Step response outputs with integrated PID controller.

TABLE III. OPTIMIZATION TECHNIQUES COMPARISON

Optimization	Metrics	Value
Step Input - I compensation (1/s)	Rise Time	2.3 s
	Peak Time	7.95 s
	Overshoot	0
Step Input - PID Controller [26]	Rise Time	0.00425 s
	Peak Time	0.0067 s
	Overshoot	0.0604

V. CONCLUSION

This study successfully discussed a proposed design for a hypergravity simulation platform speed and axis control system (HPSACS) for determining plant growth behavior and

characteristics while being influenced by hypergravity. Through a maximum determined hypergravity of 25g needed for the design, the torque was determined to be 0.36 N-m for a Yanmis AC Gear Motor with a governor for motor speed adjustment. This paper also provided CAD model visualizations for the hypergravity platform with dimensions, components, and sensor placements. The speed control system of the platform was based on a second order transfer function for its control, with necessary graphs shown as well which were generated using MATLAB. The graph of the transfer function was found out to have a high natural frequency and is ideally undamped with a high percent overshoot. The results of the speed control system analysis with step, ramp, and parabolic inputs, have shown that the most optimized system is the step input implemented with I compensation (1/s) as it has performed best in eliminating the steady-state error as well as with maintaining consistent amplitude in the graphs. Lastly, the axis stability control system was discussed in terms of its working principle and main components. The researchers recommend the in-depth analysis of an axis stability control system for future studies, since centrifuge motors have a wide range of applications. Future research can focus on expounding on the feasibility of the axis-balancing system proposed in this study that utilized the concept of water distribution and displacement.

ACKNOWLEDGEMENT

This study is supported by the Intelligent Systems Laboratory and the Office of the Vice President for Research and Innovation of De La Salle University.

REFERENCES

[1] J. A. Pandith, S. Neekhra, S. Ahmad, and R. A. Sheikh, “Recent developments in Space Food for Exploration Missions: A Review,” *Life Sciences in Space Research*, Sep. 2022. doi: https://doi.org/10.1016/j.lssr.2022.09.007

[2] J. Fischer, K. Schoppmann, and C. Laforsch, "Life History Responses and Feeding Behavior of Microcrustacea in Altered Gravity – Applicability in Bioregenerative Life Support Systems (BLSS)," in Microgravity Science and Technology, vol. 29, pp. 241-249, 2017. doi: 10.1007/s12217-017-9545-x.

[3] G. Ruyters and M. Braun, “Plant biology in space: Recent accomplishments and recommendations for future research,” Plant Biology Journal, vol. 16, 2014, pp. 4-11. doi: https://doi.org/10.1111/plb.12127

[4] C. Urbaniak et al., “Microbial Tracking-2, a metagenomics analysis of bacteria and fungi onboard the International Space Station,” *Microbiome*, vol. 10, no. 100 2022. doi: https://doi.org/10.1186/s40168-022-01293-0

[5] P. Zhang, J. Yan, Z. Liu, H. Yu, R. Zhao and Q. Zhou, “Extreme conditions affect neuronal oscillations of cerebral cortices in humans in the China Space Station and on Earth,” *Commun Biol*, vol. 5, no. 1041, 2022. doi: https://doi.org/10.1038/s42003-022-04018-z

[6] B. S. Dewitt, “Gravity,” Advances in Space Science and Technology, vol. 6, 1964, pp. 1-37. doi: https://doi.org/10.1016/B978-1-4831-9964-1.50009-X

[7] Z. Ma, “Spatial heterogeneity analysis of the human virome with Taylor’s power law,” Computational and Structural Biotechnology Journal, vol. 19, 2021, pp. 2921-2927. doi: https://doi.org/10.1016/j.csbj.2021.04.069.

[8] B. Dunbar, “The pull of hypergravity,” NASA. [Online]. Available: https://www.nasa.gov/missions/science/hyper.html.

[9] M. Fois, L. Ridolfi, and S. Scarsoglio, “In silico study of the posture-dependent cardiovascular performance during parabolic flights,” *Acta Astronautica*, vol. 200, 2022, pp. 435-447. doi: https://doi.org/10.1016/j.actaastro.2022.08.018.

[10] C. Deziel, “Gravitational factors of our eight planets,” Sciencing, 2020. [Online]. Available: https://sciencing.com/gravitational-factors-eight-planets-8439815.html.

[11] A. Kume et al., “How plants grow under gravity conditions besides 1 g: perspectives from hypergravity and space experiments that employ bryophytes as a model organism,” Plant Molecular Biology, vol. 107, 2021, pp. 279–291. doi: https://doi.org/10.1007/s11103-021-01146-8

[12] L. G. Izzo et al., "Interaction of gravitropism and phototropism in roots of Brassica oleracea," in Environmental and Experimental Botany, vol. 193, 2022, no. 104700, doi: 10.1016/j.envexpbot.2021.104700.

[13] B. Mshelmbula and G. Akomolafe, “Preliminary Investigation on the Effect of Centrifugal Force on Germination and Early Growth of Maize (Zea mays L.),” Transactions on Science and Technology, vol. 6, no. 4, 2019, pp. 328-333.

[14] M. Sathasivam et al., “Novel hypergravity treatment enhances Root Phenotype and positively influences physio-biochemical parameters in bread wheat (Triticum aestivum L.),” *Genomics*, vol. 114, 2022. doi: https://doi.org/10.1016/j.ygeno.2022.110307.

[15] K. Y. Kamal, R. Herranz, J. J. van Loon, and F. J. Medina, “Simulated microgravity, Mars gravity, and 2G hypergravity affect cell cycle regulation, ribosome biogenesis, and epigenetics in Arabidopsis cell cultures,” *Genomics*, vol. 111, 2019, pp. 1956-1965. doi: https://doi.org/10.1016/j.ygeno.2019.01.007.

[16] C. Mastrandrea and L. Vico, “Centrifugation and Hypergravity in the Bone,” R. Narayan, Ed., Encyclopedia of Biomedical Engineering, Elsevier, 2019, pp. 59-69, doi: https://doi.org/10.1016/B978-0-12-801238-3.99919-7

[17] J. Shi, H. Gu, C. Shi and T. Ma, "Design of Servo Control System for Medical Centrifuge Based on Fuzzy Neural Network," 2022 4th International Conference on Intelligent Control, Measurement and Signal Processing (ICMSP), 2022, pp. 491-494, doi: 10.1109/ICMSP55950.2022.9858955.

[18] J. Pramudijanto, A. Ashfahani, A. Fatoni and S. A. Nugroho, "PLC-Based PID-Predictive Controller Design for 3-Phase Induction Motor on Centrifugal Machine for Sugar Manufacturing Process," 2015 International Conference on Advanced Mechatronics, Intelligent Manufacture, and Industrial Automation (ICAMIMIA), 2015, pp. 49-52, doi: 10.1109/ICAMIMIA.2015.7508001.

[19] J. Tang, “Eliminate Motor Speed Fluctuations Caused By Input Voltage or Load Variance,” *Oriental motor*, 2019. [Online]. Available: https://blog.orientalmotor.com/eliminate-motor-speed-fluctuations-due-to-input-voltage-or-load-variance

[20] P. Gnaciński, D. Hallmann, A. Muc, P. Klimczak, and M. Pepliński, “Induction Motor Supplied with Voltage Containing Symmetrical Subharmonics and Interharmonics,” *Energies*, vol. 15, 2022. doi: https://doi.org/10.3390/en15207712

[21] B.D. Postma, “Robust Constrained Optimization Approach to Control Design for International Space Station Centrifuge Rotor Auto Balancing Control System,” *nasa.gov*, Patent JSC-CN-9030, 2005.

[22] F.H. Stephenson, “Centrifugation,” Calculations for Molecular Biology and Biotechnology (3rd Edition), F.H. Stephenson, Ed., Academic Press, 2016, pp. 431-438. doi: https://doi.org/10.1016/B978-0-12-802211-5.00012-6.

[23] “Amazon.com: AC Gear Motor, 220V 6W asynchronous motor M206-402 single ...,” Amazon. [Online]. Available: https://www.amazon.com/Asynchronous-M206-402-Deceleration-Adjustable-Governor/dp/B07T4PCNBS.

[24] M.C. Vlachou, “Subcooled flow boiling in horizontal and vertical macro-channel under Earth-gravity and hyper-gravity conditions,” International Journal of Heat and Mass Transfer, vol. 133, 2019, pp. 36-51. doi: https://doi.org/10.1016/j.ijheatmasstransfer.2018.12.086.

[25] T. Russomano, M. R. Rizzatti, R. P. Coelho, D. Scolari, D. De Souza and P. Pra-Veleda, "Effects of simulated hypergravity on biomedical experiments," in IEEE Engineering in Medicine and Biology Magazine, vol. 26, no. 3, pp. 66-71, May-June 2007, doi: 10.1109/MEMB.2007.364932.

[26] Y. Wang, H. Zhang, Z. Han, and X. Ni, “Optimization Design of Centrifugal Pump Flow Control System Based on Adaptive Control.” *Processes*, vol. 9, 2021. doi: https://doi.org/10.3390/pr9091538.

[27] R. Concepcion II, S. Lauguico, J. Alejandrino, A. Bandala, E. Sybingco, R. R. Vicerra, E. Dadios, and J. Cuello, “Adaptive Fertigation System Using Hybrid Vision-Based Lettuce Phenotyping and Fuzzy Logic Valve Controller Towards Sustainable Aquaponics,” *Journal of Advanced Computational Intelligence and Intelligent Informatics*, vol. 25, no. 5, pp. 610-617, 2021. doi: 10.20965/jaciii.2021.p0610.

[28] H. Aquino, R. Concepcion, A. Bandala, C. H. Mendigoria, O. J. Alajas, E. Dadios, and J. Cuello, “Fuzzy Logic Controlled Motor Speed in Rotating Aquaponics Based on Lactuca sativa Leaf Chlorosis and Necrosis and Environment Temperature,” *2021 IEEE 13th International Conference on Humanoid, Nanotechnology, Information Technology, Communication and Control, Environment, and Management (HNICEM)*, 2021. doi: 10.1109/HNICEM54116.2021.9731945.